

# High-performance Second-Generation Controlled Current Conveyor CCCII and High Frequency Applications

Néjib Hassen, Thouraya Ettaghzouti, Kamel Besbes

**Abstract**—In this paper, a modified CCCII is presented. We have used a current mirror with low supply voltage. This circuit is operated at low supply voltage of  $\pm 1V$ . Tspice simulations for TSMC 0.18 $\mu m$  CMOS Technology has shown that the current and voltage bandwidth are respectively 3.34GHz and 4.37GHz, and parasitic resistance at port X has a value of 169.32 $\Omega$  for a control current of 120 $\mu A$ .

In order to realize this circuit, we have implemented in this first step a universal current mode filter where the frequency can reach the 134.58MHz. In the second step, we have implemented two simulated inductors: one floating and the other grounded. These two inductors are operated in high frequency and variable depending on bias current  $I_0$ . Finally, we have used the two last inductors respectively to implement two sinusoidal oscillators domains of frequencies respectively: [470MHz, 692MHz], and [358MHz, 572MHz] for bias currents  $I_0$  [80 $\mu A$ , 350 $\mu A$ ].

**Keywords**—Current controlled current conveyor CCCII, floating inductor, grounded inductor, oscillator, universal filter.

## I. INTRODUCTION

In recent years, the current conveyor has improved especially for high operating frequencies, low power and low supply voltage. The concept of circuit current controlled conveyor CCCII was introduced in 1995 [1]. These circuits based on modern electronics allow the design of many electronic functions as well as the voltage mode instead of the current mode. These circuits represent a logical evolution of second generation current conveyor. They become used in high frequency applications filtering [2]-[5] and, oscillator [6]. The second generation current controlled conveyor has three port networks X, Y and Z. the relation between terminal voltage and current is given by the following matrix equation:

$$\begin{bmatrix} I_y \\ V_x \\ I_z \end{bmatrix} = \begin{bmatrix} 0 & 0 & 0 \\ 1 & R_x & 0 \\ 0 & \pm 1 & 0 \end{bmatrix} \times \begin{bmatrix} V_y \\ I_x \\ V_z \end{bmatrix} \quad (1)$$

The plus and minus signs in the third specified the polarity of the current conveyor (CCCII+, CCCII-). Due to the

N. Hassen is with the University of Monastir, Faculty of Sciences of Monastir, Tunisia, Boulevard de l'Environnement 5000 Monastir (phone: +21673 500 276; fax: +21673 500 278; (e-mail: nejib.hassen@fsm.rnu.tn).

T. Ettaghzouti is with the Faculty of Sciences of Monastir, Tunisia, Boulevard de l'Environnement 5000 Monastir (phone: +21673 500 276; fax: +21673 500 278; (e-mail: thourayataghzouti@yahoo.fr).

K. Besbes is with the Faculty of Sciences of Monastir, Tunisia, Boulevard de l'Environnement 5000 Monastir (phone: +21673 500 276; fax: +21673 500 278; (e-mail: Kamel.besbes@fsm.rnu.tn).

architecture used for the design of CCCII, the circuit will introduce parasitic elements. The characteristic equation has become:

$$\begin{bmatrix} I_y \\ V_x \\ I_z \end{bmatrix} = \begin{bmatrix} Y_y & 0 & 0 \\ \beta & Z_x & 0 \\ 0 & \pm \alpha & Y_z \end{bmatrix} \times \begin{bmatrix} V_y \\ I_x \\ V_z \end{bmatrix} \quad (2)$$

On the terminal Y and Z, two impedances  $Z_y$  and  $Z_z$  are specific to a parallel resistor with a capacitor. The impedance  $Z_x$  on terminal X is a parasitic resistor  $R_x$ . Where  $\alpha$  and  $\beta$  denotes respectively current and voltage gains.

In this article, we have improved the current controlled conveyor. Subsequently, we will use it to implement a current mode universal filter. Second, we will use it to produce two inductors: floating and tied to ground. Based, on these last two experiences, we have made two oscillators functioning at high frequency.

## II. NEW CCCII CONFIGURATION

The circuit current controlled conveyors CCCII classic introduced by [7]-[11] is shown in Fig.1.a. In intention to ameliorate bandwidth in current mode of this circuit, we present two current mirrors FVF (M8, M9, and M14) and (M12, M13, M16) which works in low voltage and characterized by low input impedance [12-15] (Fig.1.b). The two current mirrors can duplicate the current in the borne X on to the borne Z. The transistors M14 and M16 are used to adjust the linearity of the transfer characteristic of two mirrors of the output current and have currents in the paths equal X and Z ( $I_z = I_x = I_{d2} - I_{d4}$ ).

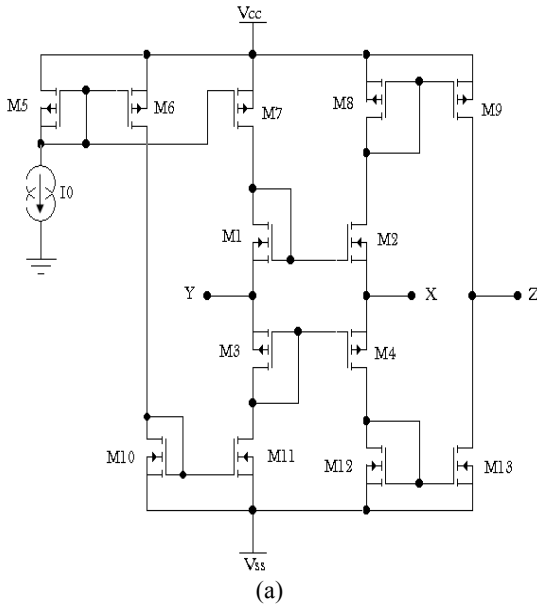
The second property of CCCII is a voltage follower between terminal X and Y. the last pair is linked together by a mixed trans-linear loop (M1, M2, M3, M4).

$$V_{xy} = (V_{GS3})_P - (V_{GS4})_P = (V_{GS1})_N - (V_{GS2})_N \quad (3)$$

$$\text{With: } (V_{GS})_N = \sqrt{\frac{(I_d)_N}{\frac{1}{2} \mu_n C_{ox} \left(\frac{W}{L}\right)_N}} + V_{THn}$$

$$\text{and } (V_{GS})_P = -\sqrt{\frac{(I_d)_P}{\frac{1}{2} \mu_p C_{ox} \left(\frac{W}{L}\right)_P}} + V_{THp}$$

The current through transistors M1 and M3 is equal to  $I_0$ . In this case, the potential difference  $V_{xy}$  is equal to:



$$V_x \cong V_y + \frac{I_x}{\sqrt{2I_0C_{ox}} \left( \sqrt{\mu_p \left( \frac{W}{L} \right)_P} + \sqrt{\mu_n \left( \frac{W}{L} \right)_N} \right)} \quad (6)$$

By identifying the characteristic equations CCCII circuit, we have:

$$R_x = \frac{I}{\sqrt{2I_0C_{ox}} \left( \sqrt{\mu_p \left( \frac{W}{L} \right)_P} + \sqrt{\mu_n \left( \frac{W}{L} \right)_N} \right)} \quad (7)$$

If  $\mu_p \left( \frac{W}{L} \right)_P = \mu_n \left( \frac{W}{L} \right)_N$

The expression of input resistance becomes:

$$R_x = \frac{1}{\sqrt{8C_{ox}\mu \frac{W}{L}} I_0} \quad (8)$$

To achieve a current controlled conveyor with negative transfer (CCCII-) we just need to reverse the current in the terminal Z. This inversion is carried out in two additional current mirrors (M1P, M2P) and (M1N, M2N) whose entries are crossed [16]-[19] (Fig.2).

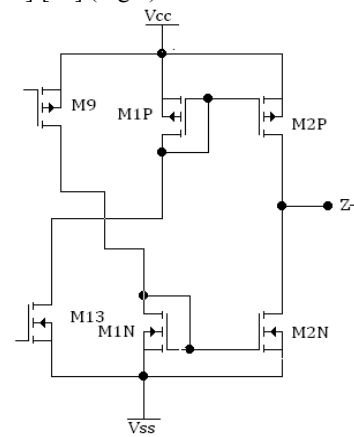
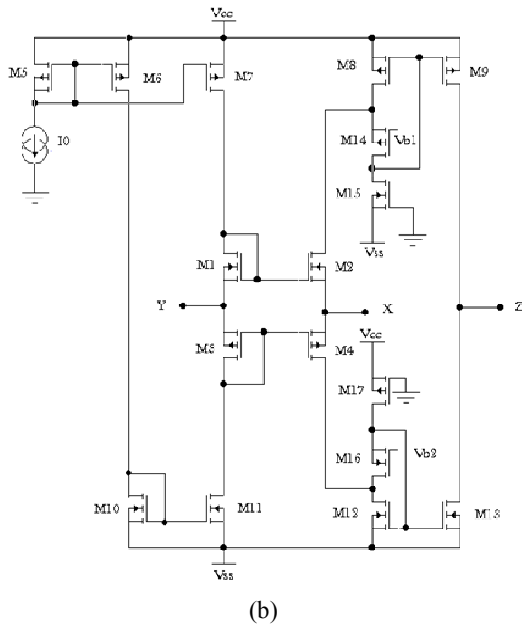


Fig. 2 Block circuit output current controlled conveyor transfer negative

Fig. 1 Circuit current controlled conveyor CCCII (a) Classic (b) Modified

$$V_{xy} = (V_{GS1})_N - (V_{GS2})_N = \sqrt{\frac{I_0}{\frac{1}{2}\mu_n C_{ox} \left( \frac{W}{L} \right)_N}} - \sqrt{\frac{(I_{d2})_N}{\frac{1}{2}\mu_n C_{ox} \left( \frac{W}{L} \right)_N}} \quad (4)$$

$$V_{xy} = (V_{GS3})_P - (V_{GS4})_P = -\sqrt{\frac{I_0}{\frac{1}{2}\mu_n C_{ox} \left( \frac{W}{L} \right)_P}} + \sqrt{\frac{(I_{d4})_P}{\frac{1}{2}\mu_p C_{ox} \left( \frac{W}{L} \right)_P}} \quad (5)$$

By determining relationships  $(I_{d2})_N$  and  $(I_{d4})_P$  according to  $I_0$  and  $V_{xy}$  from (4) and (5) and applying the relationship  $I_x = (I_{d2})_N - (I_{d4})_P$  and after taking everything into account we find:

#### A. Simulation Results of CCCII

The results are optimized by the size of transistors summarized in table I and II for a bias current  $I_0$  of 120μA and a supply voltage of ±1V. These different schemes are simulated using Tspice based BSIM3v3 transistor model for the TSMC 0.18μm CMOS process available from MOSIS [20].

TABLE I  
DIMENSIONS OF TRANSISTORS OF CLASSIC CCCII

Transistors	W / L
M1, M2	60 μm / 0.18 μm
M3, M4	90 μm / 0.18 μm
M5, M6	20 μm / 0.18 μm
M7	22 μm / 0.18 μm
M8, M9	28 μm / 0.18 μm
M10, M11	2 μm / 0.18 μm
M12, M13	17 μm / 0.18 μm

TABLE II  
DIMENSIONS OF TRANSISTORS OF AMENDED CCCII

Transistors	W /L
M1, M2	60 $\mu\text{m}$ /0.18 $\mu\text{m}$
M3, M4	90 $\mu\text{m}$ /0.18 $\mu\text{m}$
M5, M6	20 $\mu\text{m}$ /0.18 $\mu\text{m}$
M7	22 $\mu\text{m}$ /0.18 $\mu\text{m}$
M8, M9	10 $\mu\text{m}$ /0.18 $\mu\text{m}$
M10, M11	2 $\mu\text{m}$ /0.18 $\mu\text{m}$
M12, M13	8 $\mu\text{m}$ /0.18 $\mu\text{m}$
M14	22 $\mu\text{m}$ /0.18 $\mu\text{m}$
M15	0.55 $\mu\text{m}$ /0.18 $\mu\text{m}$
M16	12 $\mu\text{m}$ /0.18 $\mu\text{m}$
M17	1.52 $\mu\text{m}$ /0.18 $\mu\text{m}$

### B. Simulation Static

The Fig.3.a represents the characteristic transfer of output current  $I_z$  according to  $I_x$  in the range  $\pm 0.7\text{mA}$ . The linearity error is shown in Fig.3.b. It does not exceed 0.8% in the range  $\pm 0.35\text{mA}$  for the improved circuit. In contrast, the reference circuit, this error is much greater approximation of 5% over the same interval. The change in input resistance as a function of bias current  $I_0$  is shown in Fig.4.

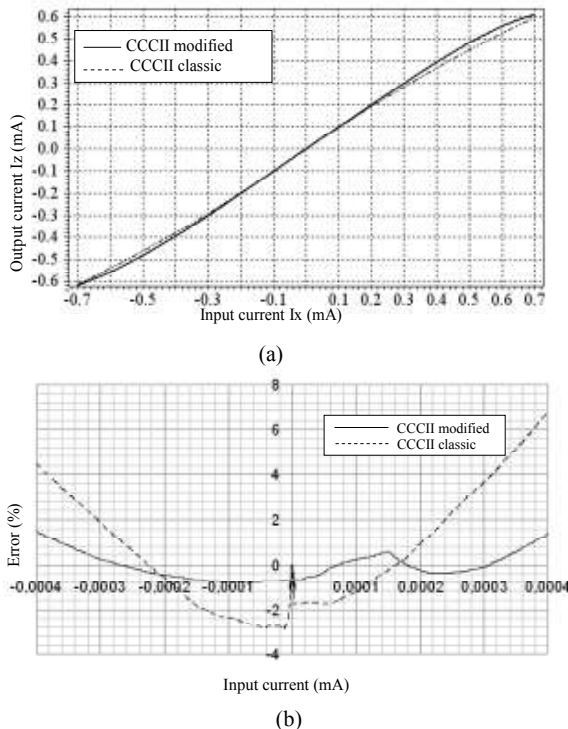


Fig. 3 (a) Variation of the output current  $I_z$  on function input current  $I_x$  (b) Variation of error as a function of input current

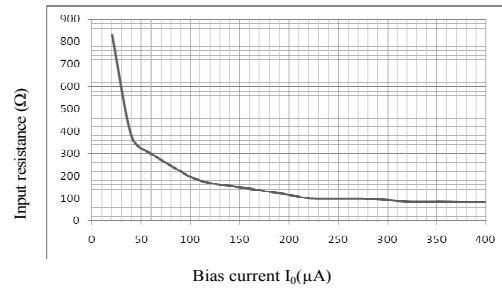


Fig. 4 Input resistance  $R_x$  as a function of bias current  $I_0$

Fig. 5 shows the variation of the voltage  $V_x$  vs. voltage  $V_y$ . It shows a good linearity in the interval  $[-0.45\text{V}, 0.45\text{V}]$ .

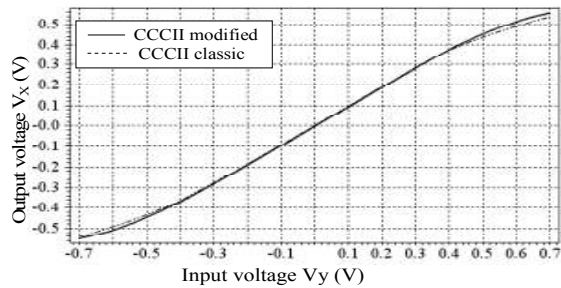


Fig. 5 Variation of output voltage  $V_x$  as a function of input voltage  $V_y$

### C. Simulation AC

Dynamic simulation is for a resisting load of  $1\text{k}\Omega$ . The frequency response of the current gain is shown in Fig.6.a. The bandwidth of the current gain at  $-3\text{dB}$  is  $3.34\text{GHz}$  instead of  $1.45\text{GHz}$ . Dynamic simulation mode voltage (Fig.6.b) gives a bandwidth of  $4.37\text{GHz}$  and a static gain of  $0.948$ . In Table 3, we have synthesized all the results of circuit simulation with the modified circuit of [8], [9], [11].

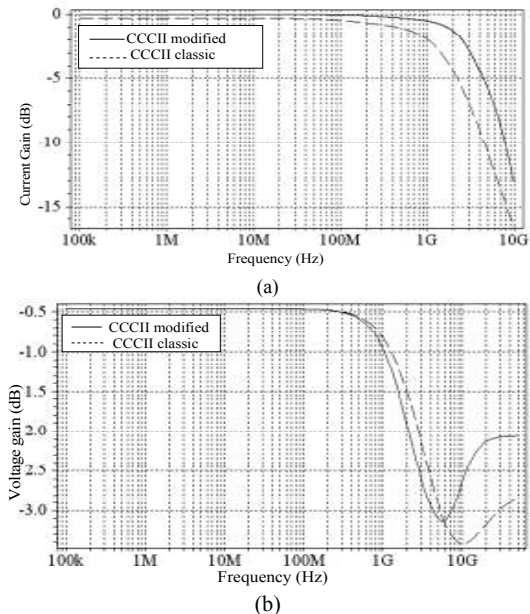


Fig. 6 (a) Current Gain as a function of frequency (b) Voltage gain as a function of frequency

TABLE III  
SIMULATION RESULTS OF CIRCUIT CCCII

	Modified circuit	Classic circuit
Technology	0,18 $\mu$ m TSMC	0,18 $\mu$ m TSMC
Bias voltage (Vcc-Vss)	2V	2V
Voltage Gain	0.948	0.948
Current gain	1	0.97
Bandwidth current $F_{CI}$	3.34GHz	1.45GHz
Bandwidth voltage $F_{cv}$	4.37GHz	5.38GHz
Error voltage ( $\pm 0.4V$ ) (%)	1.5	2,3
Error current ( $\pm 0.35mA$ ) (%)	0.8	5.16
Input resistor $R_x$	169.32 $\Omega$	196 $\Omega$
Input Impedance ( $R_y//C_y$ )	5.67K $\Omega$ //164fF	8.12K $\Omega$ //149fF
Output impedance ( $R_z//C_z$ )	6.81K $\Omega$ //37.5fF	0.876K $\Omega$ //108.01fF
THD at 1 MHz @ 0.3mA	0.24%	0.86%
THD at 1 MHz @ 0.3V	0.41%	0.47%

## III. APPLICATIONS

## A. Universal Filter

Circuit current conveyors are widely used in filtering applications. In recent years, several studies have been made specifically to improve the universal filter [2]-[5], [21]-[31]. We will use three circuit current controlled conveyors multi-output (MOCCII) (Fig.7) to achieve a universal filter current-mode [7].

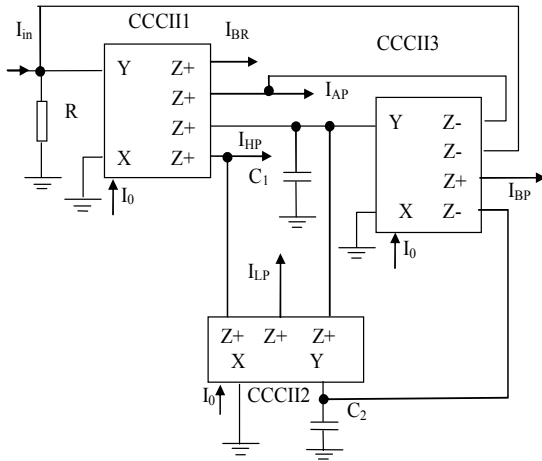


Fig. 7 Diagram of universal filter based on three MOCCII

The transfer functions of the universal filter: Low-pass, High-pass, Band-pass, Notch and All-pass are given respectively by the following expressions

$$\frac{I_{LP}}{I_{in}} = \frac{R}{R_{x1}} \frac{-I}{p^2 + p \frac{R}{R_{x1}R_{x3}C_1} + \frac{I}{R_{x2}R_{x3}C_1C_2}} \quad (9)$$

$$\frac{I_{HP}}{I_{in}} = \frac{R}{R_{x1}} \frac{p^2}{p^2 + p \frac{R}{R_{x1}R_{x3}C_1} + \frac{I}{R_{x2}R_{x3}C_1C_2}} \quad (10)$$

$$\frac{I_{BP}}{I_{in}} = \frac{R}{R_{x1}} \frac{p \frac{I}{R_{x3}C_1}}{p^2 + p \frac{R}{R_{x1}R_{x3}C_1} + \frac{I}{R_{x2}R_{x3}C_1C_2}} \quad (11)$$

$$\frac{I_{BR}}{I_{in}} = \frac{R}{R_{x1}} \frac{p^2 + \frac{I}{R_{x2}R_{x3}C_1C_2}}{p^2 + p \frac{R}{R_{x1}R_{x3}C_1} + \frac{I}{R_{x2}R_{x3}C_1C_2}} \quad (12)$$

$$\frac{I_{AP}}{I_{in}} = \frac{R}{R_{x1}} \frac{p^2 - p \frac{I}{R_{x3}C_1} + \frac{I}{R_{x2}R_{x3}C_1C_2}}{p^2 + p \frac{R}{R_{x1}R_{x3}C_1} + \frac{I}{R_{x2}R_{x3}C_1C_2}} \quad (13)$$

The proper frequency ( $f_0$ ) and the gain ( $G_0$ ) of the current mode universal filter are given by the following terms:

$$f_0 = \frac{I}{2\pi\sqrt{R_{x2}R_{x3}C_1C_2}} \quad (14)$$

$$G_0 = R / R_{x1} \quad (15)$$

To confirm the theoretical results obtained, we have performed simulations based on CMOS technology Tspice with TSMC 0.18 $\mu$ m and with a voltage bias of  $\pm 1V$ . The bias currents of CCCII three circuits are equal to 120 $\mu$ A. The values of passive components used are  $C_1=C_2=15$ pF and  $R=R_x$ . Subsequently, we have obtained a center frequency of 67,45MHz (Fig.8). In the contrast with the calculated theoretical value which is about 62.7MHz.

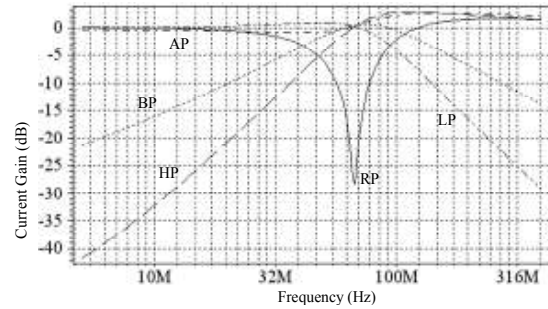
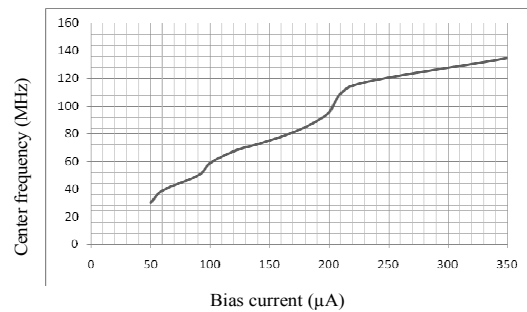


Fig. 8 Result of simulation of the module universal filter

The variation of  $f_0$  based bias current  $I_0$  is shown in Fig.9, with  $C_1=C_2=15$ pF.

Table IV shows the comparison of our results with other work on the current-mode universal filter.

Fig. 9 Change in frequency as a function of bias current  $I_0$ TABLE IV  
COMPARISON OF RESULTS OF UNIVERSAL FILTER WITH OTHER WORK

Ref	Information about the circuit	Numbers of active elements	Center frequency	Quality factor
[2]	0.5 $\mu$ m CMOS Spice $V_{CC}=-V_{SS}=1.5V$	4-DOICCI	10MHz	0.707
[3]	Rspice	3-MOCCII	110KHz	1
[5]	0.35 $\mu$ m TSMC H-Spice $V_{CC}=-V_{SS}=1.65V$	3-MOCCII	1.27MHz	1
Our results	0.18 $\mu$ m CMOS T-Spice $V_{CC}=-V_{SS}=1V$	3-MOCCII	134.58MHz	1

### B. Implementing an inductance

This problem has drawn the attention of many researchers. They have decided to make inductors based on active elements such as current conveyors, resistors and capacity. In this section, we present the creation of types of inductors, floating and related to ground, based on CCCII circuit modified.

#### 1. Floating inductor

Scheme of a floating active inductor using four CCCII+ [33]-[35] is shown in Fig.10.

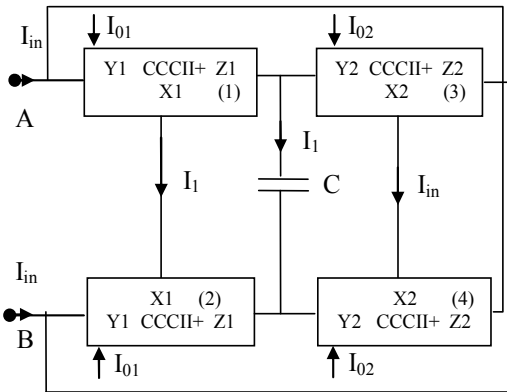


Fig. 10 Realization of floating inductance using four CCCII

The circuits CCCII 1 and 2 are biased by an identical current  $I_{01}$ , so that the capacitance  $C$  is covered by the same current. Similarly, the conveyor CCCII 3 and 4 are biased by  $I_{02}$  to have equal currents in A and B.  $R_{x1}$  is the parasitic resistance associated with the CCCII1 and 2 for the current  $I_{01}$ . Similarly,  $R_{x2}$  is the parasitic resistance associated with the CCCII3 and 4 for the current  $I_{02}$ .

$$V_{AB} = 2 R_{x1} I_l \quad (16)$$

$$V_l = \frac{I}{pC} I_l = 2 R_{x2} I_{in} \quad (17)$$

$$V_{AB} = p(2R_{x1})(2R_{x2})CI_{in} \quad (18)$$

$$L = (2R_{x1}) \times (2R_{x2})C \quad (19)$$

#### 2. Inductor connected to ground

Subsequently, based on [33]-[37], we have introduced another inductor based two current conveyor, one with positive transfer and the other with negative transfer and capacity.

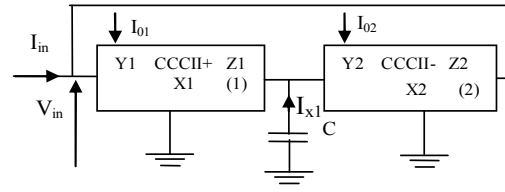


Fig. 11 Realization of an inductor connected to ground

The implementation of this inductance is illustrated in Fig.11. Taking into account the presence of parasitic resistors  $R_{x1}$  and  $R_{x2}$ :

$$V_{in} = V_{x1} = -R_{x1} I_{x1} \quad (20)$$

$$V_{y2} = V_{x2} = \frac{-I}{jC\omega} I_{x1} = R_{x2} I_{in} \quad (21)$$

According to equation (21), we have:

$$I_{x1} = -jR_{x2}C\omega I_{in} \quad (22)$$

The confusion of two expressions (20) and (22) gives:

$$V_{in} = j R_{x1} R_{x2} C \omega I_{in} \quad (23)$$

The input impedance is given by the following expression:

$$Z_{in} = \frac{V_{in}}{I_{in}} = j R_{x1} R_{x2} C \omega \quad (24)$$

It is equivalent to an inductance  $L$  for:

$$L_{eq} = R_{x1} R_{x2} C \quad (25)$$

### 3. Simulation results

In both structures, we have minimized the number of circuits used. We have used only the conveyors current to single output and only one capacity. Both inductors have an operating frequency zone and  $L$  values vary with bias current  $I_0$ . At each change in bias current  $I_0$ , we have found the area of operation frequency with an accuracy of  $\pm 5$  degrees of phase (table 5).

TABLE V  
THE VALUES OF INDUCTORS ACCORDING TO THE BIAS CURRENT  $I_0$

$I_0$ ( $\mu\text{A}$ )	Inductance connected to ground		Floating inductance	
	Frequency (MHz)	L( $\mu\text{H}$ )	Frequency max (MHz)	L ( $\mu\text{H}$ )
10	98.56-120.46	0.2830	24.07	0.0705
20	120.36-152.11	0.1410	45.66	0.0804
30	135.31-181.31	0.0844	66.99	0.0882
60	177.8-238.25	0.0270	170.42	0.102
80	216.1-295.27	0.0155	172	0.1025
90	220.36-301.1	0.0161	184.93	0.104
100	242.9-301.1	0.0158	212.32	0.1035
120	252.6-325.5	0.0092	252.93	0.107
130	266.77-334.07	0.00924	300.61	0.109
140	273.18-338.32	0.00775	305.14	0.11
150	276.03-345.92	0.00785	311.53	0.1090
160	287.35-361.94	0.00777	315.5	0.1086
180	301.33-373.58	0.00629	316.96	0.1082
200	324.22-401.35	0.00504	728.62	0.117
220	329.39-409.4	0.005	701.46	0.1168
250	344.7-423	0.0036	719.46	0.144
280	354.42-436.6	0.00358	726.11	0.1132
300	361.86-439.2	0.00357	731.14	0.1124
320	363.36-440.5	0.0035	1180	0.116
350	376.2-456.78	0.003	1200	0.115

### C. Sinusoidal Oscillator

We have given the importance of oscillators in the field of signal processing; many researchers have proposed many structures to improve their frequency performance, low power and low voltage. The proposed oscillator circuit based on an operational amplifier is shown in Fig.12.

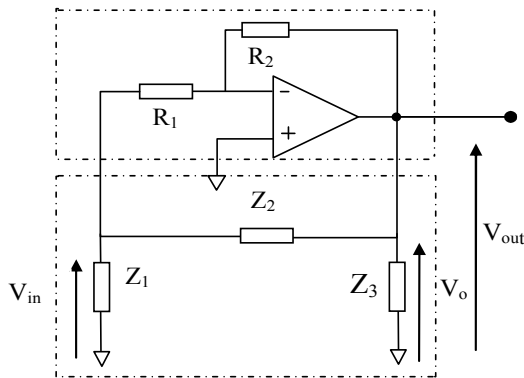


Fig.12 Implementation of an oscillator

Based on the equivalent circuit, the network reaction has as input impedance:

$$Z_{in} = Z_3 // (Z_2 + Z_1) = \frac{Z_3 (Z_2 + Z_1)}{Z_1 + Z_2 + Z_3} \quad (26)$$

The transfers function of the amplifier:

$$H = \frac{V_o}{V_{in}} = \frac{A_0 V_{in} \frac{Z_{in}}{Z_{in} + R_s}}{V_{in}} = \frac{A_0 Z_{in}}{R_s + Z_{in}} \quad (27)$$

With  $A_0$ : The gain of the direct chain. ( $A_0 = -\frac{R_2}{R_1}$ ).

$R_s$ : The output resistance characteristic of the amplifier.

The transfer function of the chain reaction is given by

$$K = \frac{V_{in}}{V_o} = \frac{Z_1}{Z_1 + Z_2}$$

According to the Barkhausen condition  $H \times K = 1$ .

We have:

$$A_0 Z_3 Z_1 = R_s (Z_1 + Z_2 + Z_3) + Z_3 (Z_2 + Z_1),$$

With  $Z_i = j X_i, i = 1, 2, 3$

The oscillation condition becomes;

$$-A_0 X_3 X_1 = j R_s (X_1 + X_2 + X_3) - X_3 (X_2 + X_1)$$

In our case  $A_0 < 0$ , by identifying:

$A_0 X_1 = -X_3$ ,  $X_1$  and  $X_3$  have the same sign as in both similar components

$X_1 + X_2 + X_3 = 0$ , the second condition requires  $X_2$

component of a different nature.

Based on some work [38]-[40], we have transformed the oscillator circuit of Fig.12 based conveyor CCCII as shown in Fig.13. This figure shows two types of oscillators: the first based on an inductor connected to ground (Fig.13.a) and the second based on a floating inductance (Fig.13.b). We used the same reactors studied previously.

A basis of an inductor connected to ground, this circuit has an oscillation frequency and gain:

$$f_0 = \frac{1}{2\pi \sqrt{(L_1 + L_2) \cdot C}} \quad (28)$$

$$A_0 = -\frac{L_2}{L_1} = -\frac{R_2}{R_1} \quad (29)$$

A basis of a floating inductor, the circuit has an oscillation frequency and gain:

$$f_0 = \frac{1}{2\pi \sqrt{\frac{C_1 C_2}{C_1 + C_2} L}} \quad (30)$$

$$A_0 = -\frac{C_1}{C_2} = -\frac{R_2}{R_1} \quad (31)$$

We performed simulations with a supply voltage of  $\pm 1V$ . The choice of components is as follows:  $C = 100nF$  to the first circuit and  $C_1 = C_2 = 0.1 pF$  for the second with the condition  $R_2 = 10 R_1$ . By the current variation of  $I_0$  [ $80\mu A$ ,  $350\mu A$ ], we obtained an oscillation frequency variable [ $358MHz$ ,  $572MHz$ ] and [ $470MHz$ ,  $694MHz$ ], respectively the first and second circuit (Fig.14)

For a bias current  $I_0 = 120\mu A$ , the signal of the oscillator is shown in Fig.15

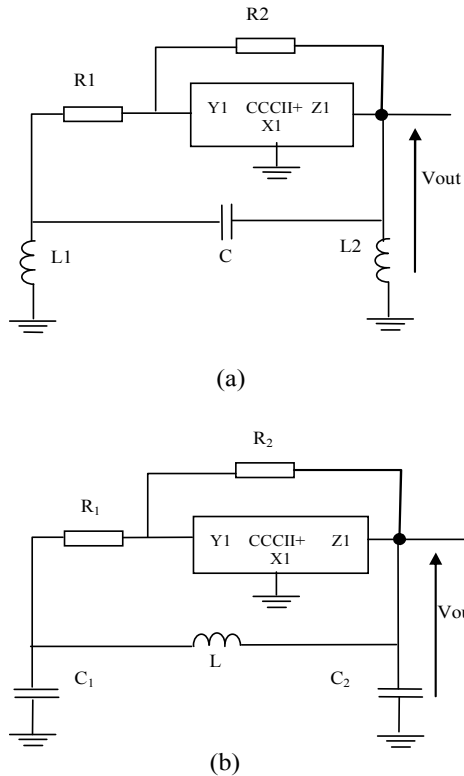


Fig. 13 Implementation of two oscillator circuit based on CCCII  
(a). a basis of an inductor connected to ground(b). a basis of a floating inductor

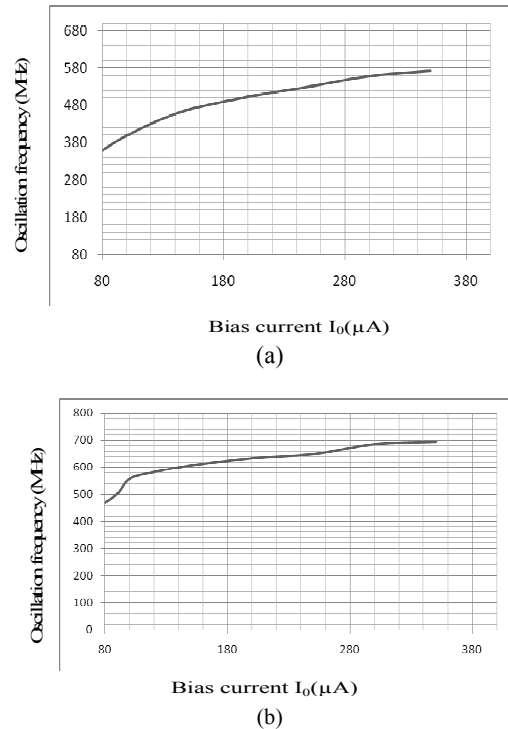


Fig. 14 Frequency of the oscillator based on current  $I_0$ (a). A basis of an inductor connected to ground(b). A basis of a floating inductor

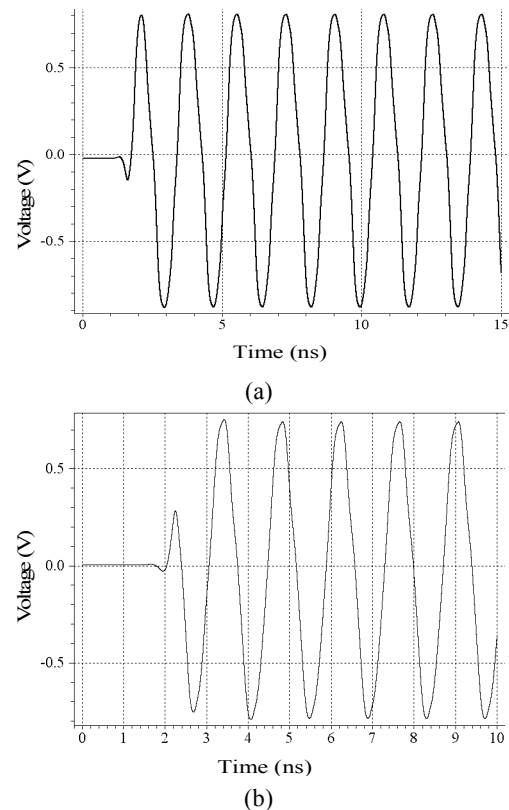


Fig. 15 Output signal of the oscillator(a). A basis of an inductor connected to ground(b). A basis of a floating inductor



## IV. CONCLUSION

In this paper we have made several improvements to the circuit current conveyor CCCII controlled using current mirrors with low supply voltage. This circuit operates at low supply voltage of  $\pm 1V$  and present to a bias current of  $120\mu A$ , a bandwidth of  $3.34GHz$  and  $4.37GHz$  respectively in current mode and voltage mode for expenses and a  $1k\Omega$  parasitic resistance  $R_x$  of  $169.32\Omega$ . Based on this circuit, we have implemented first a universal filter, current mode. The frequency can reach the  $134.58MHz$ . In the second, we have implemented two inductors, one floating and the other tied to ground, operating in high frequency and variable depending on bias current  $I_0$ . We have used the last two, respectively, to implemented two sinusoidal oscillators frequency one  $[358MHz, 572MHz]$ , second  $[470MHz, 692MHz]$  for bias currents  $I_0$   $[80\mu A, 350\mu A]$ .

## REFERENCES

- [1] A. Fabre, O. Saaid and al, "High-frequency high-Q BiCMOS current mode bandpass filter and mobile communication application". *IEEE journal of solid-state Circuits*, August 2002; vol 33, no 3, pp.614-625.
- [2] Ahmed M Soliman, "Current mode filters using two output inverting CCII", *International journal of circuit Theory and applications*. October 2008; vol 36, no7, pp.875-881
- [3] Sudhanshu Maheshwari and Iqbal A. Khan, "Novel cascaded current-mode translinear-C universal filter", *Active and Passive Electronic Components*, December 2004; vol 27 no 4, pp.215-218.
- [4] Neeta Pandey and al, "Realization of Generalized Mixed Mode Universal Filter Using CCCIs", *Journal of Active and Passive Electronic Devices*, 2009; vol 55, no 3, pp.279-293.
- [5] H. P. Chen and P. L. Chu, "Versatile universal electronically tunable current-mode filters using CCCIs", *IEICE Electron Express*, 2009; vol 6, no 2, pp.122-128.
- [6] Ozcan.S, Toker.A and al. "Single resistance controlled sinusoidal oscillators employing current differencing buffered amplifier", *Microelectronics Journal (International)*, 2000, vol31, no 3, pp.169-174.
- [7] Chunhuna Wang, Yan Zhao and al. "A New Current Mode SIMO Type Universal Biquad employing Multi-Output Current Conveyors (MOCCIs)", *Radio engineering*, April 2009, vol 18, no 1, pp.83-88.
- [8] Samir ben Salem, Mourad Fakhfakh and al. "A high performances CMOS CCII and high frequency application", *Analog Integrated Circuit and Signal Processing*, April 2006, vol 49, no 1, pp.71-78
- [9] Ercan Altuntas and Ali Toker, "Realization of voltage and current mode KHN biquads using CCCIs", *International Journal of electronics and communications*, January 2002, vol 56, no 1, pp.45-49.
- [10] Sinem Oztayfun, Selcuk Kiinc and Aem Celebi, "A new electronically tunable phase shifter employing current-controlled current conveyors", *AEU-International journal of Electronics and communications*, March 2008, vol 62, no 3, pp.228-231.
- [11] Hervé Barthelemy, Matthieu Fillaud and al, "CMOS inverters based positive type second generation current conveyors", *Analog Integrated Circuit and Signal Processing*, February 2007, vol 50, no 2, pp.41-146..
- [12] Torralba A, Carvajal RG and al. "New output stage for low supply voltage high performance CMOS current mirrors", *Circuits and Systems, 2003 ISCAS '03. Proceedings of the 2003*, 20 Jun 2003, vol 1, pp.269-272
- [13] Sauerbrey J, Wang J and al. "A 0.6V multi-VT current mirror differential OTA", *International Symposium on Signals, Circuits and Systems (ICECS)*, August 2005, vol 1, pp.279-282.
- [14] Néjib Hassen, Houda Bdiri Gabbouj and Kamel Besbes, "Low-voltage high-performance current mirrors Application to linear voltage-to-current converter", *International Journal of circuit Theory and Applications*, January 2011; vol 39, no 1, pp.47-60..
- [15] Maneesha Gupta, Prashant Aggarwal and al., "Low voltage current mirrors with enhanced bandwidth", *Analog Integrated Circuit and Signal Processing*, 2009, vol 52, no 7, pp.1276-1279.
- [16] A. Fabre, H. Amrani and H.Barthelemy, "Novel class AB first generation current conveyor", *Circuits and Systems II: Analog and Digital Signal Processing IEEE*, 06 August 2002; vol 46, no 1, pp 96-98;
- [17] M.Higashinura and M.Fukui, "Novel method of realizing higher order immittance function using current conveyor", *circuit and system IEEE international*, 1998.
- [18] Kimmo Kilo, "CMOS current amplifiers speed versus Nonlinearity", Thesis Helsinki University of Technology; November 2000.
- [19] Giuseppe Ferri and Nicol Guerri, "High-valued passive element simulation using low-voltage low-power current conveyors for fully integrated applications", *Circuits and Systems II: Analog and Digital Signal Processing, IEEE*, August 2002, vol 48 no.4,
- [20] The MOSIS service, "Wafer electrical test data and spice model parameters" <http://www.mosis.org/test/>
- [21] Shen-IUAN and JIIN-LONG LEE, "Voltage-mode universal filters using two current Conveyors", *International Journal of Electronic*, 1997, vol 82 no 2, pp145-149.
- [22] Kazuhiro Nakai and Gaushi Yamamoto, "Universal biquadratic filters using current conveyors", *electronics and communication. Analog Integrated Circuit and Signal Processing*, May 2005, vol 31, no 3, pp. 1-16.
- [23] Erkan Yuce and Shahran Minaei, "Universal current-mode filters and parasitic impedance effects on the filter performances", *International journal of circuit Theory and applications*, March 2008, vol 36, no 2.
- [24] Ahmed M Soliman, "Voltage mode and current mode tow Thomas bi-quadratic filters using inverting CCII", *International journal of circuit Theory and applications*, July 2007; vol 35, no 4.
- [25] An Jerabek and kamil Vrba, "SIMO type Low-Input and High-Output impedance current mode universal filter employing three universal current conveyors", *AEU - International Journal of Electronics and Communications*, March 2009, vol 64, no 6, pp 588-593.
- [26] Jun-Wei Horng Chun-Li Hou, "Current-Mode Universal Biquadratic Filter with Five Inputs and Two Outputs Using Two Multi-Output CCIs", *Circuits, Systems, and Signal Processing*, vol 28, no 5, pp 781-792.
- [27] Ahmed M. Soliman, "Current-Mode Universal Filters Using Current Conveyors Classification and Review", *Circuits, Systems, and Signal Processing*, 2008, vol 27, no 3, pp 405-427.
- [28] Neeta Pandey and Sajal K.Paul, "A new electronically tunable current mode universal filter using MO-CCCI", *Analog Integrated Circuit and Signal Processing*, February 2009, vol 58, no 2, pp 171-178.
- [29] E. Tlelo-Cuautle and al. "Symbolic analysis of (MO)(I)CCI(II)(III)-based analog circuits", *International journal of circuit Theory and applications*, 2009.
- [30] Antonio.J, Lopez Martin and al. "A proposal for high-performance CCII-based analogue CMOS design", *International journal of circuit Theory and applications*, 2005, vol 33, no 5, pp 379-391.
- [31] George Souliotis and Ioannis Haritantis, "Current-mode filters based on current mirror arrays", *International journal of circuit Theory and applications*, 2008, vol 36, no 2, pp173-183.
- [32] Ahmed M. Soliman, "The CCII+ and the ICCII as basic building blocks in low-pass filter realizations", *International journal of circuit Theory and applications*, 2008, vol 36, no 4, pp 493-509
- [33] Dorra Sellami Masmoudi and Nadhmia Bouaziz El Feki, "A high frequency CCII based tunable floating inductance and current-mode band pass filter application", *Journal of Applied Science*, 2005, vol 5, no 8, pp 1445-1451.
- [34] Ahmed Soliman, "On the realization of floating inductors", *Nature and Science*, 2010, vol 8, no 5, pp 167-180.
- [35] H. Sedel M. Sagbas and C.Acar, "Current controllable fully integrated inductor simulator using CCCIs", *International journal of electronics*, May 2008, vol 95, no 4, pp 425-429.
- [36] Erkan Yuce and Shahram Minaei, "On the Realization of Simulated Inductors with Reduced Parasitic Impedance Effects", *Circuits, Systems, and Signal Processing*, 2009, vol 28, no 3, pp 451-465.
- [37] Chun-Li Hou and Wei-Yu Wang, "Higher-order immittance functions using current Conveyors", *Analog Integrated Circuit and Signal Processing*, November 2009, vol 61, no 2, pp 205-209.
- [38] Guillems Ganzalez, "Foundations of Oscillator Circuit Design", Publication, *Société Mathématique in France*, Paris, 2007, Book, ISBN: 2856292585.
- [39] A.S.Elwakil, S.Ozoguz and K.N.Solama, "Ring oscillator structures with explicitly separated nonlinearity", *International journal of circuit Theory and applications*, 11 Jun 2010.

- [40] Mehmet Discigil, Ali toler and al. "New Oscillator Topologies Using Inverting Second-Generation Current Conveyors", *Turkish Journal of Electrical Engineering & Computer Sciences*, 2002, vol 10, no 1..
- [41] Erkan Yuce and Oguzhan Cicekoglu, "The Effects of Non-Idealities and Current Limitations on the Simulated Inductances Employing Current Conveyors", *Analog Integrated Circuits and Signal Processing*, February 2006, vol 46 no 2, pp 103–110.



**Néjib HASSEN** was born in 1961 in Mknine, Tunisia. He received the B.S. degree in EEA from the University of Aix-Marseille I, France in 1990, the M.S. degree in Electronics in 1991 and the Ph.D. degree in 1995 from the University Louis Pasteur of Strasbourg, France. From 1991 to 1996, he has worked as a researcher in CCD digital camera design. He implemented IRDS new technique radiuses CCD noise at CRN of GOA in Strasbourg. In 1995, he joined the Faculty of Sciences of Monastir as an Assistant Professor of physics and electronics. Since 1997, he has worked as researcher in mixed-signals neural networks. Actually he is focusing on the implementation low voltage - low power circuits.



**Thouraya Ettaghzouti** was born in Tozeur, Tunisia, in 1983. She received the B.S. degree from the Faculty of Sciences of Monastir in 2008, the M.S. degree from at the same University at the Microelectronic and Instrumentation Laboratory in 2010. Actually, she is preparing the Ph.D degree. She is interested to the implementation of low voltage low power integrated circuit design.



**Kamel BESBES** was born in Monastir, Tunisia, in 1960. He received the B.S. degree from the Faculty of Sciences of Monastir in 1985, the M.S. degree from the Ecole Centrale de Lyon, Lyon, France, in 1986, the Ph.D. degree from the Institut National des Sciences Appliquées de Lyon (INSA), Lyon, in 1989, and the Doctorat d'Etat degree from the Faculty of Sciences of Tunis, Tunisia, in 1995. In 1989, he joined the Faculty of Sciences of Monastir as an Assistant Professor of physics and electronics. He is now a Professor and the Dean of the Faculty and the Head of the Microelectronics and Instrumentation Laboratory. His research work and interest are focused on microelectronics, modeling, and instrumentation.